Surface Thermal Conditions in the Western North Pacific during the ENSO Events

By Kimio Hanawa, Tomowo Watanabe, Naoto Iwasaka, Toshio Suga and Yoshiaki Toba

Department of Geophysics, Faculty of Science, Tohoku University, Sendai 980, Japan

(Manuscript received 7 September 1987, in revised form 23 April 1988)

Abstract

In order to clarify the surface thermal conditions during the ENSO events, composite analyses of the SST anomaly fields were performed over the western North Pacific, and for the mixed layer in the Kuroshio current region at sections along the 137°E line and a line over the Izu Ridge. Each winter during the 25 years from 1961 to 1985 was classified into one of four categorized winters, *i.e.*, ENSO-1 year, ENSO year, ENSO+1 year and the *other* year winters. For example, for the 1982/83 ENSO event, the 1983 winter (January through March) was regarded as the ENSO year winter. It was found that in the ENSO year winter, a well-ordered positive SST anomaly appears in a wide zonal band along the 30°N line, extending from the Asian coast to near 170°E. On the other hand, the distribution of SST anomalies in the ENSO+1 year winter is quite similar to that in the ENSO year winter with its sign reversed. During the ENSO year winter, the mixed layer in the Kuroshio current region south of Japan was thinner and warmer than those in the other three categorized winters. One of possible causes for these differences was attributed to the strength of the east Asian winter monsoon. It is relatively weaker in the ENSO year winter, compared with the other three categorized winters.

1. Introduction

It has been widely accepted that the El Niño/Southern Oscillation (ENSO) events have an impact on global atmospheric conditions through various processes, for example, the Pacific/North American (PNA) teleconnection pattern (see, *e.g.*, Horel and Wallace, 1981). During the ENSO events, the ocean is also influenced by these atmospheric phenomena. For example, Iwasaka *et al.* (1987) showed that variations in the sea surface temperature (SST) represented by the 1st mode of the Empirical Orthogonal Function (EOF) analysis, which appears strongly in the central and eastern North Pacific, are responsible for the PNA teleconnection pattern.

For ENSO events in the equatorial region, remote oceanic regions can be influenced in two ways. One, by the atmosphere as mentioned above, which has an immediate and direct influence on the upper oceanic structure by air-sea interactions, and the other by the ocean itself, whose influence will slowly appear in subsurface structures. Saiki (1986) suggested through use of a composite analysis of the SST anomaly fields that at the early stage of ENSO evens (summer), the SST lowers east of Honshu Island, Japan, while during their mature stage (winter), the SST forms positive anomalies in the area south of Japan. This may be an example of the former route. On the other hand, Yamagata *et al.* (1985) pointed out the intensification of the Kuroshio Extension and the Kuroshio Counter Current with a time lag of about 1.5 years to that of the North Equatorial Current. The variation of the latter current is considered

to be closely related to ENSO events (*e.g.*, Wyrtki, 1975). This may be an example of the latter route.

The purpose of the present study is to clarify the surface thermal conditions in the western North Pacific especially in mid-latitudes, and of the mixed layer in the Kuroshio region during ENSO events. In order to understand the generation mechanism of the SST anomaly in mid-latitudes, clarification of the relationship between ENSO events and the SST variations must be considered, since these ENSO events provide "heartbeat" to the global atmosphere as mentioned above. Up to the present, although many investigators have analyzed the SST fields, they have mainly dealt with those in the central and eastern North Pacific during ENSO events, and only a few have investigated the SST variations in mid-latitudes of the western North Pacific.

In the present study, following Wright *et al.* (1985), the ENSO phenomena are regarded as discrete events separated by periods within which the variations are of less interest. Moreover, focus is made on the winter-time thermal conditions, as a first step towards understanding winter-time SST formation, which affects the SST fields in this area in succeeding seasons (Watanabe and Hanawa, 1988).

In Section 2 the data used and the classification of winters during the analyzed period are described. Section 3 discusses the results of composite and correlation analyses of SST anomaly fields. Composite analyses of the mixed layer in the Kuroshio current region is presented in Section 4. The relationship between the east Asian winter monsoon and the ENSO events is discussed in Section 5, while Section 6 gives the conclusions and discussion.

2. Data, data processing and the definition of ENSO year winter

a. The data used

A 25-year monthly mean SST data set was compiled from the North Pacific Climate Tables which had been issued regularly by the Japan Meteorological Agency (JMA) from 1961 to 1979, and from the original tapes of marine meteorological elements gathered by the Marine Meteorological Department of the JMA from 1980 to 1985. These data are arranged on a 2°x5° (lat. x lon.) grid over the ocean area that covers the western North Pacific from 100°E to 170°W and from the equator to 60°N. Distributions of the number of the observations are described in Watanabe and Hanawa (1988). Seasonal mean SSTs were calculated from the monthly data with those for January, February and March regarded as the winter season, etc., since, in general, SSTs in mid-latitudes have minimum values in February.

The data of serial hydrographic observations along the 137°E line conducted by the JMA from 1967 to 1987, were used for analysis of the mixed layer over the Kuroshio current region. The observational line is shown in Fig. 1. Winter-time regular observations have been made from late January to early February. See Andow (1987) for details of the data, in which he presented maps of the upper ocean structures of temperature, salinity and dissolved oxygen, and

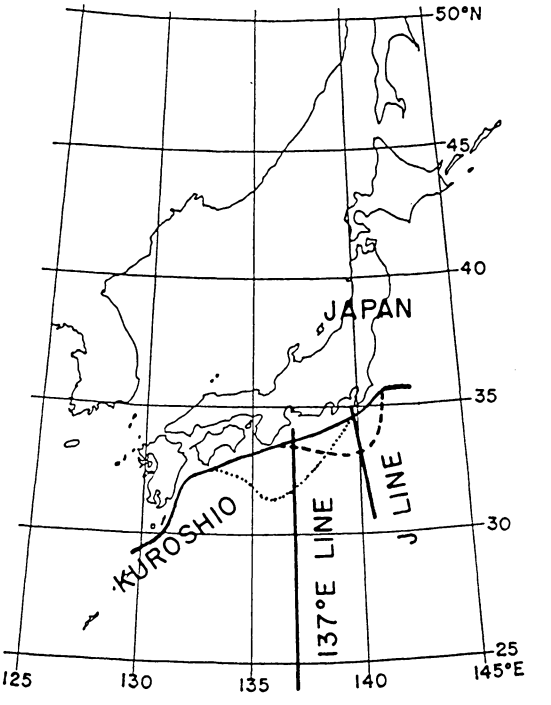

Fig. 1. Two hydrographic observational lines used for analysis of mixed layer of the Kuroshio current region: the 137°E line conducted by JMA and the J line made by the Oshima Branch of the Tokyo Fisheries Laboratory.

those of anomaly fields.

The data of serial hydrographic observations conducted by the Ohshima Branch of the Tokyo Fisheries Laboratory from 1964 to 1987 along the Izu Ridge (J line in Fig. 1) were also used. The J line consists of ten observational stations and observations were made during February and April for almost every year (Hanawa and Hoshino, 1988).

b. Definition of the ENSO year winter

Usually ENSO events are considered as events of a two-year span. Therefore, an ENSO year winter within an ENSO event can be defined as the three months of January, February and March. For example, those three months in 1983 are regarded as the ENSO year winter of the 1982/83 ENSO event.

Years of ENSO events have been listed by various authors based on various indices such as the Southern Oscillation Index (SOI). Weare (1986) used the El Niño Index (ENI), which was defined as the time coefficients of the 1st EOF for the SST anomaly in the Pacific Ocean. He listed ENSO primary years occurring during the period from 1950 to 1985 as 1957, 1965, 1972, 1976 and 1982. On the other hand, Rasmusson and Carpenter (1982), who made composite analyses for SST, wind and other elements, listed ENSO primary years as 1951, 1953, 1957, 1963, 1965, 1969 and 1972 during the period from 1950 to 1973.

In the present study, ENSO primary years for the period from 1961 to 1987 were selected as 1963, 1965, 1969, 1972, 1976, 1982 and 1986. Therefore, there are seven ENSO year winters, *i.e.*, the winters of 1964, 1966, 1970, 1973, 1977, 1983 and 1987. In addition, in the present study, all winters were classified into four categories, *i.e.*, the ENSO-1 year, ENSO year, ENSO+1 year and the *other* year winters.

c. The mixed layer in the Kuroshio current region

In general, the bottom of the oceanic upper mixed layer has been defined as the depth at which a temperature of SST-1℃ occurs (*e.g.*, Hanawa and Hoshino, 1988). For the 137°E line, the temperature of the mixed layer was regarded as that at a depth of 10m. Averages of the mixed layer temperature and thickness of the Kuroshio current region (from the Kuroshio axis to 30°N) were calculated. Here, the Kuroshio axis was determined by using the index of the 15°C isotherm at a depth of 200 m. This index for the Kuroshio axis has been widely used for the area south of Japan (*e.g.*, Kawai, 1972; Taft, 1972). Due to the southward shift of the Kuroshio axis during the Kuroshio Large Meander, the number of raw data were different from year to year. When the number of the raw data was only one (one station) for a given section, the temperature and thickness of the mixed layer for that year were not calculated.

Hanawa and Hoshino (1988) made a composite analysis of the thermal structure and mixed layer of the Kuroshio current region along the J line. They constructed the composite maps using a coordinate which had its origin on the Kuroshio axis, and described the mean state and anomaly fields for the temperature and thickness of the mixed layer in the Kuroshio current region (from 50 km south of the axis to 250 km). In the present study, this data set and the data obtained in 1987 were used.

3. Composite analyses for SST anomaly fields

a. Composite SST maps for four categorized winters

Figures 2(a) and (b) show composite maps for the SST anomaly field, and that for the SST anomaly field normalized by the standard deviation at each grid point, respectively, for the ENSO year winter. Note that the composite map for the normalized SST anomaly field can represent the relative strength of the anomaly field within ranges of the SST anomaly variations at each grid point. Therefore, the figures complement each other. In the ENSO year winter, strong and well-ordered patterns of anomalies with positive values appear in a zonal band along the 30°N line from the Asian coast almost to the international date line. On the other hand, in the western equatorial area strong negative anomalies appear, while in the central equatorial area positive anomalies exist. The arrangement of these SST anomalies in the equatorial region is well-known feature of the

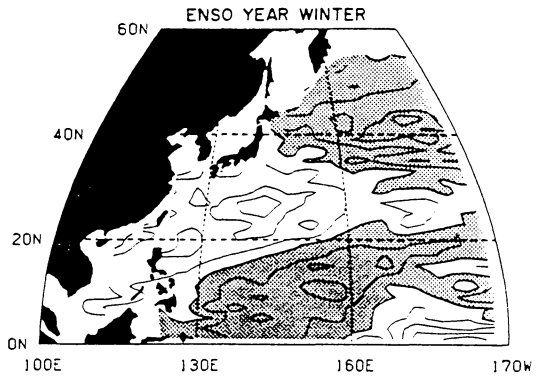

(a)

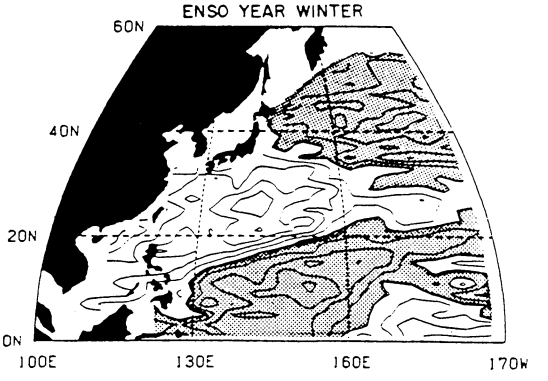

(b)

Fig. 2. Composite maps of the SST anomaly fields for the ENSO year winter. (a) SST anomaly fields. Units are ℃ and contour interval is 0.2℃. (b) SST anomaly fields normalized by the standard deviations at each grid point during 25 years. Contour interval is 0.25. Dotted areas show the regions with negative anomalies.

ENSO events (*e.g.*, Rasmusson and Carpenter, 1982; Weare, 1982; Yasunari, 1987a,b). The sea area north of the 35°N line has negative SST anomaly fields.

Figure 3 shows the composite SST anomaly fields for the remaining three categorized winters. For the ENSO+1 and −1 year winters, the SST anomalies have opposite signs compared with those in the ENSO year winter. In particular, the anomaly pattern for the ENSO+1 year winter contrasts sharply with that for the ENSO year winter. It is found that the area of the strongest response, *i.e.*, the center of action, in both categorized winters is the area around 30°N, 145°E. For the *other* year winter, the SST anomaly fields do not show these characteristic features and the anomalies themselves are weak.

For an actual individual winter, for example, winter during the 1982/83 ENSO event, patterns similar to the above composites can be observed as shown in Fig. 4. It should be noted here that in the so-called minor ENSO events, strong positive anomalies in mid-latitudes do not necessarily appear even in the ENSO year winter. For example, in the 1969/70 and 1976/77 ENSO events (not shown here), winter-time SST fields in mid-latitudes of the western North Pacific show the weak negative anomalies.

b. *Comparison with results of cluster analysis by Iwasaka et al. (1988)*

Iwasaka *et al.* (1988) classified the North Pacific into several regions in terms of the temporal similarity of monthly SST anomaly fields by using a cluster analysis. They showed that for the winter data (December, January through March in their study) the ocean area along the 30°N line from Japan to 165°E is partitioned into one cluster. Figure 5 shows the results of their regional partitioning, in which borderlines for the clusters are superposed on Fig. 2(a). Their Region A corresponds rather well with the area of positive anomalies and Region B to the negative anomalies. Regions A and B also correspond to the negative and positive anomaly pattern, respectively, in the ENSO+1 year winter as shown in Fig. 3. Therefore, it is concluded that Region A and Region B strongly reflect the SST variation relating to the ENSO events.

Furthermore, Iwasaka *et al.* (1988) pointed out that SST variations of Regions C and D are closely related to the variation of the PNA teleconnection pattern. The existence of a negative anomaly pattern in the northern North Pacific shown in Fig. 2 suggest that the PNA teleconnection pattern, in general, tends to be formed during the ENSO events.

c. *Correlation between SST and the El Niño Index proposed by Weare (1986)*

Figure 6 shows the distribution of correlation coefficients between the SST anomaly field and the El Niño Index (ENI) proposed by Weare (1986). The period analyzed is from 1962 to

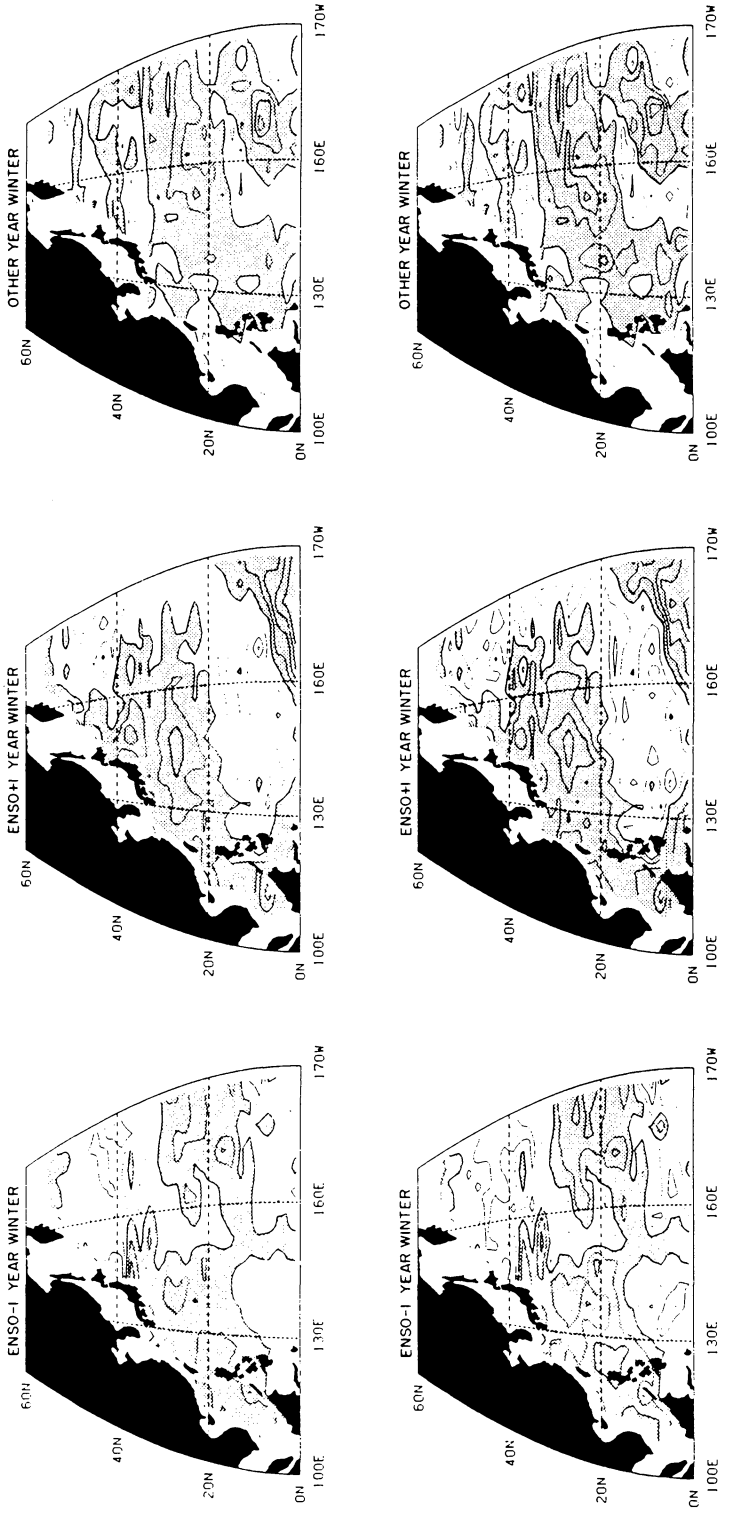

Fig. 3. As in Fig. 2, except for the other three categorized winters, *i.e.*, (a) ENSO-1 year winter, (b) ENSO+1 year winter and (c) *other* year winter. Upper panels show SST anomaly fields and lower panels show normalized SST anomaly fields, respectively.

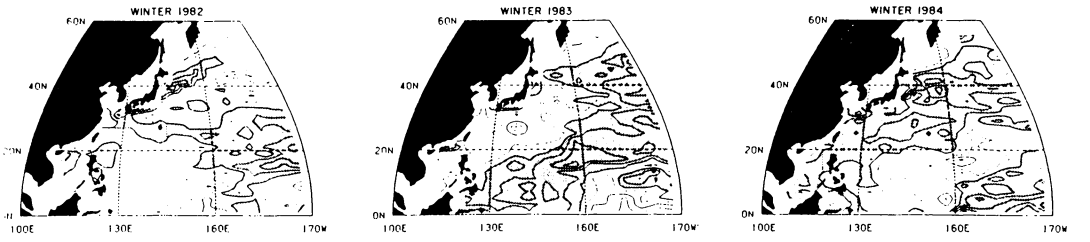

Fig. 4 Selected typical SST anomaly fields in winter for (a) 1982 (ENSO-1 year) winter, (b) 1983 (ENSO year) winter and (c) 1984 (ENSO+1 year) winter during the 1982/83 ENSO event. Contour interval is 0.5℃.

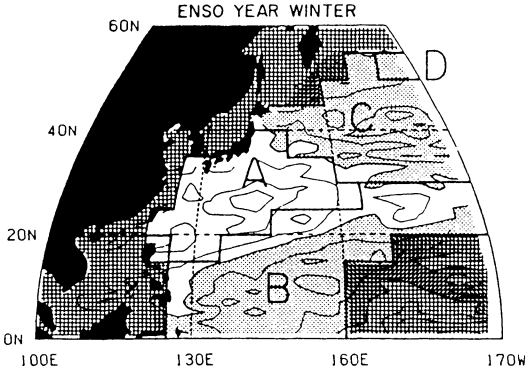

Fig. 5. Regions (A-D) specified by cluster analyses made by Iwasaka *et al.* (1988) for winter-time monthly SSTs of 5°×5° (lat. × lon.) sea area in the North Pacific during 11 years from 1969 through 1979. The borderlines are superposed on SST anomaly fields in the ENSO year winter (Fig. 2(a)). The cross striped areas show the regions excluded in their analyses.

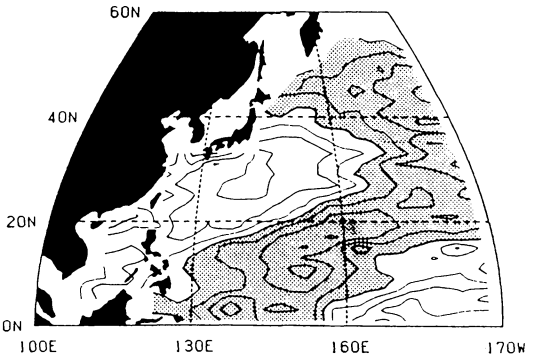

Fig. 6. Distribution of correlation coefficients between the wintertime SST anomaly fields and the El Niño Index proposed by Weare (1986). Since ENIs have large positive values during the ENSO events, the areas with positive correlation coefficients correspond to the regions with positive SST anomalies in the ENSO year winter. Contour interval is 0.20. The 95% significant level of correlation coefficient by the *t*-test is about 0.42.

1983. Winter-time ENI was obtained by averaging those of December, January and February. Since the number of data is 22, there are 20 degrees of freedom and the significance level of 95% by the *t*-test is approximately 0.42 (Hays, 1981). Not only the pattern of the positively correlated area in mid-latitudes but patterns for the whole area correspond remarkably well to those shown in Fig. 2. Also they coincide with the clusters defined by Iwasaka *et al.* (1988). This figure shows the relationship between the strength of the SST anomaly field and the strength of the ENSO events, and therefore gives more support to the anomaly patterns presented in Fig. 2.

From the results and the discussion described in subsections *b* and *c* above, it can be concluded that the anomaly patterns that occur during the ENSO year and ENSO+1 year winters are well-ordered features in the western North Pacific.

d. Temporal evolution and decay of SST anomaly fields

Figure 7 shows composite maps of normalized SST anomaly fields for six seasons beginning with the ENSO-1 year spring and ending with the ENSO year autumn, excluding the ENSO year winter. The seasons of the ENSO-1 year, winter (from Fig. 3) through autumn show negative SST anomaly fields south and east of Japan. In the ENSO year winter (Fig. 2), however, positive anomalies suddenly appear in the area from 20°N to 40°N and from the Asian coast to the eastern

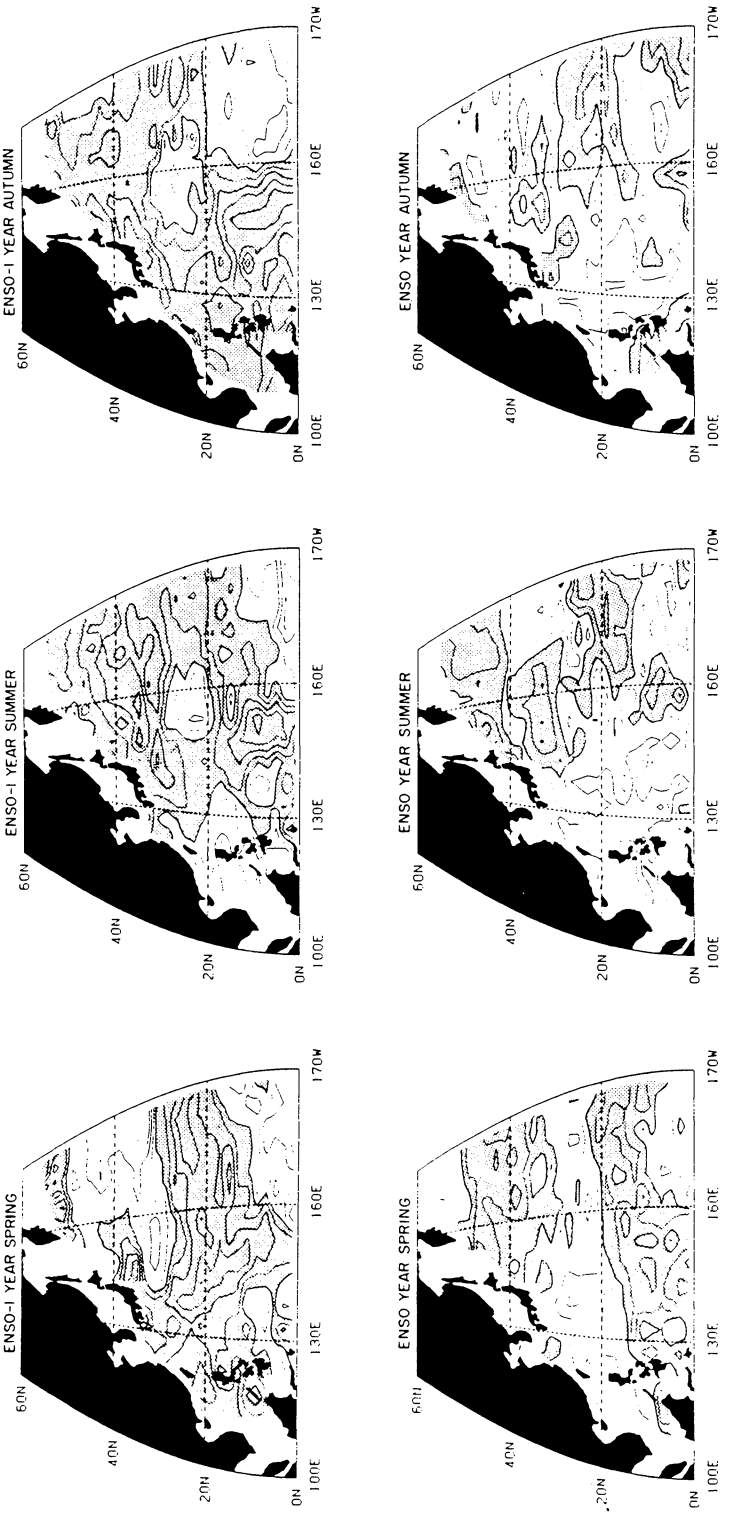

Fig. 7. As in Fig. 2(a), except for composite maps of normalized SST anomaly fields for six seasons from the ENSO-1 year spring to the ENSO year autumn, excluding the ENSO year winter.

end of the analyzed area and continue through spring. In summer, over the ocean east of Japan, negative anomalies appear, and in autumn, relatively small scale anomalies of both signs appear. However, in the ENSO+1 year winter (Fig. 3), strong negative anomalies appear in mid-latitudes of the western North Pacific.

On the basis of a correlation analysis, Watanabe and Hanawa (1988) pointed out that the SST fields in mid-latitudes of the western North Pacific tend to be refreshed in every winter. The present temporal sequence of the SST anomaly fields confirms these findings.

4. The mixed layer in the Kuroshio current region during the ENSO events

It is expected that since positive SST anomalies appear in a large area in mid-latitudes during the ENSO year winter, the mixed layer in the Kuroshio current region is warmer compared with those of the other three categorized winters. In this section, the mixed layer in the Kuroshio current region is examined, along two observational lines (see Fig. 1).

Figure 8 shows time series of the anomalies for mixed layer temperature and thickness along the 137°E and J lines. The mean values were calculated from available data for an individual line and for an individual month for the J line. Mixed layer mean values of the temperature and thickness are 19.8°C and 188m, respectively, for the 137°E line and those for February and April of the J line are 18.7°C, 19.3°C and 240m and 183m, respectively (Hanawa and Hoshino, 1988). The Kuroshio current along the section of the J line has a large variability in temperature and thickness of the mixed layer with ranges (standard deviation) of about 0.8°C and 70 m, respectively. Note that, since years with no data are different from one line to the other, the anomalies of one time series can not be directly compared with the other time series.

Figure 9 shows the relationship between the mixed layer temperature and thickness for the four categorized winters. Although three panels do not necessarily completely show the same tendency among the ENSO+1/−1 year and the *other* year winters, they do show that, in general, the mixed layer in the Kuroshio current region is

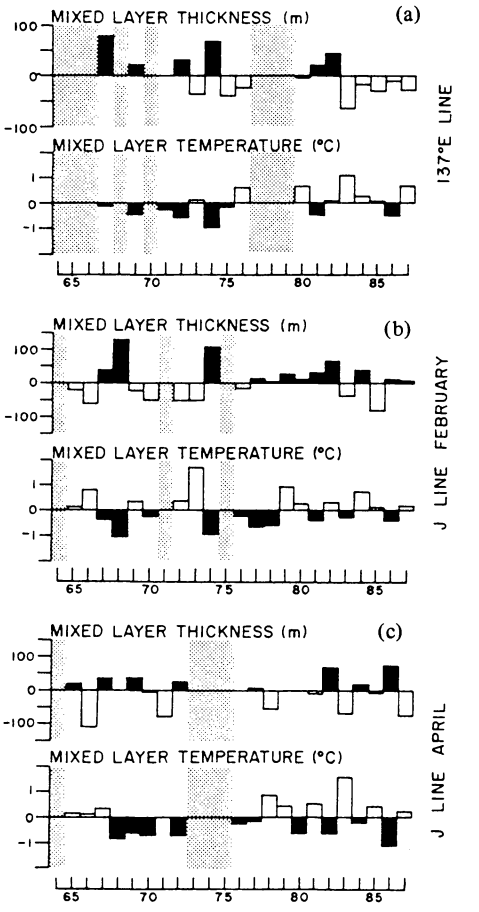

Fig. 8. Time series of the mixed layer temperature and thickness in the Kuroshio current region. (a) The 137°E line, (b) the J line in February and (c) the J line in April. The years represented by dotts show those with no available data, and mean values were obtained for the rest.

thinner and warmer during the ENSO year winter, while those in the other three categorized winters are thicker and colder. At the 137°E line, the difference between the ENSO year winter and the three categories reaches about 0.8°C in temperature and about 60m in thickness. The standard deviation for each element is larger along the J line than the 137°E line. This may reflect that the flow structure of the Kuroshio current is, to some extent, influenced by the bottom topography of the Izu Ridge, as suggested by Ohtsuka (1985).

Here, it is worthwhile to note the following relationship between temperature and thickness

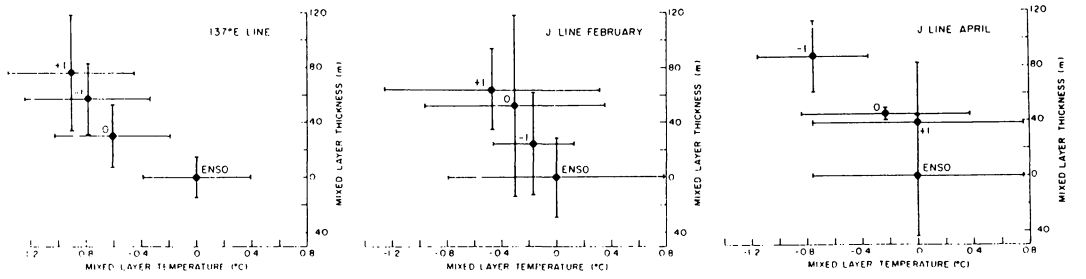

(a) (b) (c)

Fig. 9. Relationship between the mixed layer temperature (horizontal axis) and thickness (vertical axis) of the Kuroshio current region for the four categorized winters. (a) The 137°E line, (b) the J line in February and (c) the J line in April. Symbols of ENSO, +1, −1 and O denote the ENSO year, ENSO+1/−1 year and the *other* year winters, respectively. The horizontal and vertical bars denote twice the standard deviations. Note that since years of the data used for this calculation are different among three data sets. Values of the ENSO year winter were used as the origin of the coordinates.

of the mixed layer. In general, temperature and thickness of the mixed layer are positively correlated in the equatorial regions, especially in the central and eastern regions (*e.g.*, see Donguy *et al.*, 1984). However, in mid-latitudes, they are negatively correlated, as described here. This difference depends on the mean upwelling at the bottom of the mixed layer. Upwelling, which is a three-dimensional process, is essential for the mixed layer evolution in an equatorial region, while it can be neglected in mid-latitudes where one-dimensional processes are relatively dominant.

5. East Asian winter monsoon in the ENSO year winter

Watanabe and Hanawa (1988) discussed the relationship among anomaly fields of air temperature, SST in the western North Pacific, the MOnsoon Index (MOI, the sea level pressure difference between Nemuro, Japan and Irkutsk, USSR) and Southern Oscillation Index (SOI, the sea level pressure difference between Darwin and Tahiti). First, they postulated that the MOI is a useful index of the east Asian winter monsoon, and showed that a high MOI corresponds to low air temperature in the Japan Islands. In addition, they showed that winter-time SST anomaly fields in the ocean east and south of Japan have a high correlation which both the MOI and SOI. The MOI has a relatively high correlation with the SST in the area near the Asian continent and in the zonal band along 30°N, while the SOI shows a high correlation with the SST in the offshore region centered at 30°N, 140°E. Moreover, they combined both indices and found a new index, *i.e.*, MSI (MOI+SOI), that can represent conditions of the SST fields much better than an individual index. This result means that the SST fields in mid-latitudes of the western North Pacific are influenced by atmospheric conditions in both mid- to high-latitudes and an equatorial region. Their analytical conclusions were based on the fact that the *strength* of the atmospheric forcing plays an important role in generating the SST anomaly fields.

The MOI, SOI and MSI were averaged for the four categorized winters. Each index was defined from mean values of December, January and February, following Watanabe and Hanawa (1988). Figure 10 shows the averages for the four categorized winters from the data during the period from 1961 to 1987. Although the standard deviations were large, it was concluded that the strength of the east Asian winter monsoon is relatively weak for the ENSO year winter compared with that for the other three categorized winters. However, there was also no remarkable difference among the ENSO+1/−1 year and the *other* year winters.

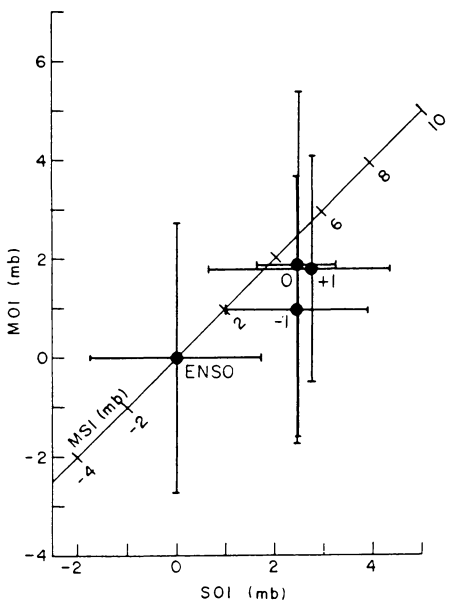

Fig. 10. As in Fig. 9, except for SOI and MOI for the four categorized winters. The inclined line in the figure denotes the axis for MSI.

6. Conclusions and discussion

In order to clarify surface thermal conditions in the western North Pacific and mixed layer condition in the Kuroshio current region during ENSO events, composite analyses for SST anomaly fields and temperature and thickness for the mixed layer in the Kuroshio current region along the 137°E and J lines were performed.

The main results can be summarized as follows.

(1) In the ENSO year winter, the SST fields have positive anomalies in a wide zonal band along the 30°N line that extends from the Asian coast to near 170°E. The position of the maximum anomaly is found around 30°N and 145°E. This area responds strongly to ENSO events.

(2) SST anomaly patterns for the ENSO year and ENSO+1 year winters, which are relatively strong compared with the other two categorized winters, coincide with the results of cluster analysis by Iwasaka *et al.* (1988).

(3) SST anomalies formed in the ENSO year and ENSO+1 year winters persist to spring and to some extent even to autumn. However, the SST fields tend to be reversed in the next winter. This confirms the findings of Watanabe and Hanawa (1988).

(4) The mixed layer in the Kuroshio current region is thinner and warmer in the ENSO year winter, compared with the other three categorized winters.

(5) One of possible causes for these variations can be attributed to the strength of the east Asian winter monsoon: it is weaker in the ENSO year winter, compared with the other three categorized winters.

The duration of the data used in the present study is only 25 years for the SST, and 21 and 24 years for the data along the 137°E and J lines, respectively. Since the four categorized winters consist of only 4 to 6 data sets each, the composite values have relatively large standard deviations for most of elements described here. Although large standard deviations may result from the scarcity of the data, another reason may be that the signals of the ENSO events are essentially contaminated by independent processes occurring in mid-latitudes of the western North Pacific, compared with those in the equatorial region.

Zhao and McBean (1986) analyzed the ocean-atmosphere heat (long wave radiation, latent and sensible heats) transfers for the northern North Pacific, and made correlation analyses between the SOI and the fluxes of several specified regions. The correlation coefficients between the SOI and fluxes of the Kuroshio region (sea south of Japan) did not exceed a significant level for winter as well as for all seasons. However, they did not investigage short wave radiation, *i.e.*, oceanic heat gain. Therefore, to estimate the air-sea net heat exchange, and to clarify relationship among heat fluxes, the east Asian winter monsoon (and/or MSI) and SST fields during ENSO events is left for future studies. The authors believe that this is very important and interesting work, since it is closely related to problems concerning the formation of the Subtropical Mode Water (Hanawa, 1987; Suga *et al.*, 1988), which is widely distributed in the subsurface layer along the Kuroshio in the western interior of the subtropical gyre.

In the present study, each winter was

classified into one of four categories, *i.e.*, the ENSO year, ENSO+1/−1 year and the *other* year winters. However, large differences among the ENSO+1/−1 year and the *other* year winters could not be found for most of the elements treated except for the SST anomaly field, *i.e.*, the mixed layer temperature and thickness in the Kuroshio current region, and MOI, SOI and MSI. Therefore, the appearance of a strong negative SST anomaly in the ENSO+1 year winter suggests that less of the heat is transported to the mid-latitudes by the Kuroshio in the second year during an ENSO events. This may also mean that an anti-ENSO phase (cold event) in mid-latitudes does not appear clearly in atmospheric elements. The difference in the manner of the appearance of ENSO and anti-ENSO phases in mid-latitudes is one of the problems to be solved in a future study.

As mentioned in the Introduction, the present study was mainly concerned with a direct response of the ocean *via* the atmosphere during ENSO events. For an indirect response *via* the ocean with some time lag, *i.e.*, oceanic advection of signals, more careful treatment of the oceanic subsurface data will be needed.

Acknowledgments

The authors would like to express their sincere thanks to the Marine Meteorological Department of the JMA for kindly providing the necessary data. They also thank two anonymous reviewers for their useful comments on the manuscript. This study was made as part of OMLET (Chairman: Y. Toba), one of the Japanese WCRP activities, which was financially supported by Japanese Ministry of Education, Science and Culture.

References

Andow, T., 1987: Year-to-year variation of oceanographic subsurface section along the meridian of 137°E. *Oceanogr. Mag.*, **37,** 47-73.

Donguy, J.-R., A. Dessier, G. Eldin, A. Morliere and G. Meyers, 1984: Wind and thermal conditions along the equatorial Pacific. *J. Mar. Res.*, **42,** 103-121.

Hanawa, K., 1987: Interannual variation in the wintertime outcrop area of Subtropical Mode Water in the western North Pacific ocean. *ATMOSPHERE-OCEAN*, **25,** 358-374.

——— and I. Hoshino, 1988: Temperature structure and mixed layer of the Kuroshio over the Izu Ridge. To appear in *J. Mar. Res.*

Hays, W.L., 1981: *Statistics* (3rd ed.). Holt-Saunders International Editors, pp.723.

Horel, J.D. and J.M. Wallace, 1981: Planetary-scale atmospheric phenomena associated with Southern Oscillation. *Mon. Wea. Rev.*, **109,** 813-829.

Iwasaka, N., K. Hanawa and Y. Toba, 1987: Analysis of SST anomalies in the North Pacific and their relation to 500mb height anomalies over the Northern Hemisphere during 1969-1979. *J. Meteor. Soc. Japan*, **65,** 103-114.

———, ——— and ———, 1988: Partition of the North Pacific Ocean based on similarity in temporal variations of the SST anomaly. *J. Meteor. Soc. Japan*, **66,** 433-443.

Kawai, H., 1972: Hydrography of the Kuroshio Extension. In: Kuroshio – its physical aspects, ed. by H. Stommel and K. Yoshida, Univ. Tokyo Press, Tokyo, p.235-352.

Ohtsuka, K., 1985: Characteristics of the Kuroshio in the vicinity of the Izu Ridge. *J. Oceanogr. Soc. Japan*, **41,** 441-451.

Rasmusson, E.M. and T.H. Carpenter, 1982: Variations in tropical sea surface temperature and surface wind fields associated with the Southern Oscillation/El Niño. *Mon. Wea. Rev.*, **110,** 354-384.

Saiki, M., 1986: Abnormal sea condition and atmospheric condition. *Bull. Jap. Soc. Fish. Oceanogr.*, **50,** 142-144 (in Japanese).

Suga, T., K. Hanawa and Y. Toba, 1988: Subtropical Mode Water in the 137°E section. Submitted to *J. Phys. Oceanogr.*

Taft, B., 1972: Characteristics of the flow by the Kuroshio south of Japan. In: Kuroshio – its physical aspects, ed. by H. Stommel and K. Yoshida, Univ. Tokyo Press, Tokyo, p.165-216.

Watanabe, T. and K. Hanawa, 1988: Relationship between SST of the western North Pacific and Monsoon and Southern Oscillation indices. To be submitted to *Ocean-Air Int.*

Weare, B.C., 1982: El Niño and tropical Pacific Ocean surface temperatures. *J. Phys. Oceanogr.*, **12,** 17-27.

———, 1986: Extension of an El Niño index. *Mon. Wea. Rev.*, **114,** 644-647.

Wright, P.B., T.P. Mitchell and J.M. Wallace, 1985: Relationships between surface observations over the global oceans and the southern oscillation. *NOAA Data Rep. ERL PMEL-12*, pp61.

Wyrtki, K., 1975: El Niño – The dynamic response of the equatorial Pacific Ocean to atmospheric forcing. *J. Phys. Oceanogr.*, **5,** 572-584.

Yamagata, T., Y. Shibao and S.-I. Umatani, 1987: Interannual variability of the Kuroshio extension and its relation to the southern oscillation/El Niño. *J. Oceanogr. Soc. Japan*, **41,** 274-291.

Yasunari, T., 1987a: Global structure of the El

Niño/Southern Oscillation. Part I. El Niño Composites. *J. Meteorol. Soc. Japan*, **65**, 67-80.

———, 1987b: Global structure of the El Niño/Southern Oscillation. Part II. Time evolution. *J. Meteorol. Soc. Japan*, **65**, 81-102.

Zhao, Y.P. and G.A. McBean, 1986: Annual and interannual variability of the North Pacific ocean-to-atmosphere total heat transfer. *ATMOSPHERE-OCEAN*, **24**, 265-282.

ENSOイベント期間中の西部北太平洋表層水温場

花輪 公雄・渡邊 朝生・岩坂 直人・須賀 利雄・鳥羽 良明

（東北大学理学部地球物理学教室）

ENSOイベント期間中の西部北太平洋における表層水温場の状態を明らかにするため，海面水温アノマリと，東経137度線および伊豆海嶺上の測線（J線）における黒潮領域の混合層に対する合成図解析を行った。1961年から1985年までの25年間の冬季を，ENSO－1年，ENSO年，ENSO＋1年，他の年の四つのカテゴリに分類した。たとえば，1982／83年ENSOイベントでは，1983年1～3月がENSO年冬季とみなされる。解析の結果，ENSO年冬季の海面水温場には，アジア大陸から東経170度付近までの北緯30度線に沿った幅広い領域で，顕著な正のアノマリが出現することがわかった。一方，ENSO＋1年冬季の海面水温場は，符号が逆のENSO年冬季の分布と極めてよく一致しているアノマリ分布を示していた。また，ENSO年冬季の日本南方の黒潮領域は，他のカテゴリの冬季に比べ温かく薄い混合層であった。この差異を生じさせる原因のひとつとして，東アジアの冬季季節風の吹き出しの強さを挙げることができた。すなわち，ENSO年冬季の季節風の吹き出しは，他のカテゴリの冬季に比べて相対的に弱い状態となっていた。